Hittite Journal of Science and Engineering, 2022, 9 (1) 45–56
ISSN NUMBER: 2148–4171
DOI: 10.17350/HJSE19030000254

Investigation of the Interaction of the Tank Structures Exposed To Earthquake with the Soil

Asuman Isil Carhoglu
Suleyman Demirel University, Department of Civil Engineering, Isparta, Turkey

Article History:
Received: 2021/11/19
Accepted: 2022/02/28
Online: 2022/03/30

***Correspondence to**: Asuman Işıl Çarhoğlu, Suleyman Demirel University, Civil Engineering, Isparta, TURKEY*
E-Mail: isilcarhoglu@sdu.edu.tr
Phone: +90 246 211 12 15

ABSTRACT

Liquid storage tanks storing liquids such as gasoline and LNG are very important structures. These tructures can be damaged because of the loss of strength that may occur due to external influences. It is known that a considerable amount of damage occurred in tank structures, which are one of the industrial structures, happened during the earthquakes occurred in the past. Determining the behavior of the buildings which are under the effect of an earthquake is very important in order to prevent damage to the building during a possible earthquake. The behavior of structures built on soft soils is considerably different from that of structures constructed on a rigid soil. For this purpose, in this study, a steel tank structure was modeled by considering the different soil profiles. During modelling, an elastic spring method was used for the soil while the finite element method was used for the tank and the basic interaction of the soil and foundation structure which are exposed to earthquake loads were examined. Dynamic analyzes were carried out using the time history method by taking into consideration 11 earthquake records having the different properties. According to the results of the displacement and stress values obtained; It was observed that the values obtained in the earthquakes, whose peak ground acceleration and ground velocity are large, are higher than other earthquakes. It was seen that as the soil resistance increases, the strength of the structure increases during earthquakes.

Keywords:
The structure-soil-interaction; Liquid storage tank structures; Time history analysis; Earthquake; Spring stiffness

INTRODUCTION

Earthquakes with different characteristics have occurred all over the world for years and cause loss of life and property. Some of the largest earthquakes in the world are 1995 Kobe earthquake, 1906 San Francisco Earthquake (M = 7.9), 1989 Loma Prieta (M = 6.9), 2018 Anchorage Alaska Earthquake (M = 7.1), 2014 South Napa, California Earthquake (M = 6.0) and 2004 Northern Sumatra (M = 9.0) [1]. Up until today, many devastating earthquakes have occurred in Turkey located on an active fault line. Some of these earthquakes are 1998 Adana Ceyhan Earthquake (M_w= 6.3), 1999 Kocaeli Earthquake (M_w = 7.4), 1999 Düzce Earthquake (M_w = 7.2), 2002 Afyon-Sultandağı Earthquake ((M_w = 6.3), 2003 Bingöl Earthquake (M_w = 6.4) and 2011 Van Earthquake (M_w = 6.3) [2]. The magnitude of Kocaeli earthquake was 7.4 and it occurred at an area which was quite busy in terms of industry. This earthquake occurred in the North Anatolian fault which has a length of 1500 km and its depth of focus in the southeast of Izmit is 7 km, its depth of focus in the east of Istanbul is 80 km [1,3,4]. This strong earthquake caused great damage at Tüpraş refinery in Izmit. Many Naptha tanks were damaged in Tüpraş refinery, and 2 elevated liquid oxygen tanks collapsed at the Habas plant [3].

It is important for earthquake engineering to examine the fluid-structure-soil interaction of structures such as off-shore, suspension bridges and liquid storage tanks. The interaction of liquid-structure-soil shows variation depending on the features of the structures. For this reason, it is necessary to model such structures correctly. The liquid storage tank is widely used in industry and nuclear plants for the purpose of storing different liquids such as oil and liquefied natural gas [5]. Liquid storage tanks are exposed to earthquakes. The rigidity of the tank structures will decrease due to the low strength values that will occur in the soils during the earthquake. Therefore, it is of great importance to examine the soil structure interaction since substantial damages will occur in the structures. When the past earthquakes are analyzed, it is observed that shell buckling occurs in structures built on a flexible foundation. It is seen that the effect of the foundation in tank structures exposed to the earthquake is of great significance and it is necessary to examine the soil structure interaction. Inertia forces may occur in the system of the liquid structure system due to seismic effects forming on the bottom of the tank during the earthquake [6].

The Structure-soil interaction is known as the effect of the movements occuring in the soil due to the structure and the effect of the movement occuring in the structure due to soil as a result of the effects such as earthquakes. Kinematic and inertial interaction are involved in structure-soil interaction. Horizontal and vertical displacements occur on the soil during an earthquake. If the foundation is very rigid, kinematic interaction occurs when the ground motion will be prevented by changing the properties of the wave motion on the soil [7]. When examining the seismic performance in the buildings, it is seen that one of the most important factors related to the extension of the building period is rotation that occurs in the foundation [8,9]. The effects such as collapse and rotation occurring in the soil are ignored by assuming with the fixed base in the analysis performed for the purpose of determining the behavior of the structures exposed to the earthquakes. However, since the rigidities of soft soil are less than the hard soil, the periods of constructions built on the soft soil are longer than those of the hard soil. As the soil stiffness decreases, the structure period increases and therefore the great changes happen in the values such as deformation, displacement, base shear force and stress occuring in the structure.

Mezaini M. determined the design forces to be formed in the cylindrical tank were determined by using the SAP 2000 Program by taking account of the different soil conditions and foundation geometry. When the results were examined, it was seen that there were differences in the design forces [10]. Kianoush [5] performed the analyses by modeling as shallow and tall with the finite elements method the concrete rectangular tank structure exposed to the four ground motions in order to examine the liquid structure interaction. The base shear, moment and sloshing values were determined and compared by depending on the frequency properties of earthquakes for different soil situations [5]. Bhattacharya [11] investigated the changes in the system of the structure-soilfoundation with the increasing of the lateral natural period by considering the concrete frame structures with the different span and height. Soils with different features were designed using an elastic spring model. The changes in the values of the natural period and base shear force were examined [11]. Dutta [12] made analyses as elastic and inelastic for frame structures in low-rise different features by modelling as elastic spring the soil for the purpose of examining the soil-structure-interaction. Ghandil [13] obtained the values of the lateral displacement and the story shear force by considering nonlinear soil-structure interaction analysis of structures with different floor numbers by taking account of the different soil properties. Elasto-plastic Mohr-Coulomb model were used ELM and NFM methods during soil modeling. Meng [14] compared the values of the natural frequencies, displacement, base shear force and overturning moment of the liquid storage tanks to obtain their soil-structure interaction [14]. Dutta[15] examined the soil-structure interaction for the elevated tank structures. Zhao [16] was performed the earthquake analysis by designing a steel nuclear power plant structure with the finite element method. Time history analysis method was made in the analyzes. Dynamic analyzes were made by considering different baffle types, heights and lengths of the structure. Analyzes were performed for Kobe and El Centro earthquakes for 0, 0.2, 0.6, 0.9 and 1 height ratios of the nuclear plant. The maximum acceleration values at the top of the tank for earthquake conditions are determined according to the different height ratio. However, the comparisons were made by obtaining the displacement and stress values. Zhao [17] examined the seismic analysis of tank structures. An Arbitrary Lagrangian Eulerian (ALE) algorithm has been used to examine the liquid structure interaction. The ratio of water height to tank height and the ratio of water mass to total mass parameters are taken into account. Pressure, stress, frequency and overturning moment values of water are obtained and compared. Nicolici [18] were designed the liquid-filled containers in order to examine liquid structure interaction. Time history analysis was performed to examine the interaction between the tank wall and the liquid. The liquid effect is modeled by the mass spring method. A bidirectional FSI approach was used to examine the effect on the wall due to the water effect. In the analysis results, the values of impulsive, convective pressure, the wave height of liquid and base reaction are determined and examined. Patel [19] examined in the dynamic interaction of the fluid-structure-soil. The interaction of the fluid-structure studied by using the added mass approach of Westergaard. The fluid in the tank was dealt with as water. Hard, medium and soft soils was utilized as soil profiles by examining the interaction structure-fluid-soil. Soil was modelled as spring. In the results of the time history analysis, The values of the displacement and base shear force were obtained and compared. Seleemah [20] were performed the seismic analysis of the isolated tanks by using 3D-BASIS-ME, SAP2000 programs. Tank structures were modeled as shell element. The convective mass of the liquid and rigid mass was located in the center of tank and base of tank respectively and link element indicating rigidity was settled in the horizontal direction by modelling fluid. The values of the displacement obtained from isolated tanks were compared by using 3D-BASİS-ME and SAP 2000 programs. Livaoğlu [21] examined in interaction of the fluid-structure-soil by utilizing the mechanical and

A. I. Carhoglu/ ittite J Sci Eng, 2022, 9 (1) 45–56

finite element methods for ten tank structures on the different soil features. The values of base shear, displacement and overturning moment were obtained. Livaoğlu [22] carried out the seismic behaviour of the structure of elevated tank on different soils. The fluid in the tank was modeled with spring mass model belonging to Housner. Impulsive mass and convective mass were used for added mass approach. These masses were attached to the finite element. The water was dealt with as the fluid in the container. According to the analysis results, it was seen that the important changes in the earthquake behavior of tanks occured depending on the soil properties. At the same time, it was determined that the displacement and impulsive modes were more bigger than torsional modes.

In this study, The behavior of a tank structure under the effect of earthquake was investigated. For this reason, A tank structure and soil were designed by assuming different soil properties. The selected soil properties have different mechanic properties and the soil was designed with the equivalent elastic spring method [23]. Lineer time history analyses were performed with Sap 2000 by addressing eleven ground motion records [24].

IDEALIZATION OF THE LIQUID STORAGE TANK-SOIL SYSTEM

Idealization of The Liquid Storage Tank System

Determining the behaviors of buildings exposed to earthquake effects is an issue that should be addressed in terms of earthquake engineering. Since the seismic behaviour of tank structure is studied by taking into consideration the soil-structure interaction, the liquid storage tank have been designed as shell element through the use of SAP 2000 Programme [24]. The tank structure, with radius of 20 m and height of 14 m, was designed as shell. The elasticity module of the tank steel was measured as 2.1 10^{11} N/m^2, the unit volume weight was 7.69 kg / m^3, and the unit volume weight of the liquid was 807.9 kg/ m^3 [25]. The three-dimensional view of the tank is shown in Fig. 1.

The liquid in the tank is modeled using a mass-spring system. According to the Housner mass-spring system; The total mass of the liquid in a tank exposed to the earthquake is divided into two as M_o and M_1. A part of the liquid moves together with the tank wall during the earthquake as the tank walls move. This mass, called M_o, is rigidly connected to the tank wall at the h_0 height, as shown in Fig. 1. Oscillations occur in the rest of the water due to the movement of the tank wall, and this oscillating force is shown as M_1. Oscillating M_1 mass is attached to the tank walls with the help of a spring. In this way, hydrodynamic pressure forces are created by using the mass-spring model. In equation 1-5, R: The radius of the cylindrical tank, h: the water depth of the cylindrical tank, M: total mass, M_0: the mass at the ho height, M_1: the mass at the h_1 height. M_0 impulsive mass and M_1 sloshing mass are obtained from Equations 1 and 2. The values of h_0 and h_1 are found by Equations 3 and 4 in order to determine the dynamic pressure forces. The spring constant that connects the sloshing mass to the tank wall is obtained by Equation 5 [26, 27, 28].

$$M_0 = M \frac{\tanh 1.7R/h}{1.7R/h} \tag{1}$$

$$M_1 = M(0.6) \frac{\tanh 1.8h/R}{1.8h/R} \tag{2}$$

$$h_0 = \tfrac{3}{8} h \left\{ 1 + \propto \left[\tfrac{M}{M_1} \left(\tfrac{R}{h} \right)^2 - 1 \right] \right\} \tag{3}$$

$$h_1 = h \left[1 - 0.185 \left(\frac{M}{M_1} \right) \left(\frac{R}{h} \right)^2 - 0.56\beta \frac{R}{h} \sqrt{\left(\frac{MR}{3M_1 h} \right)^2 - 1} \right] \tag{4}$$

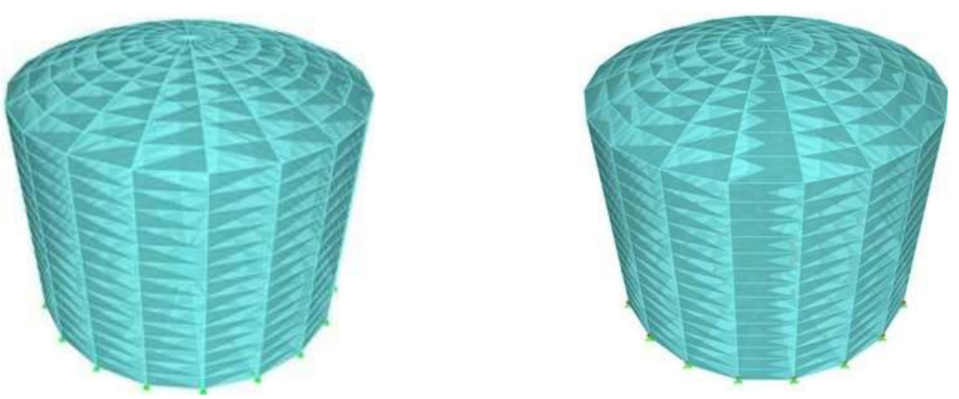

a) The structure with fixed support.

b) The structure that the soil is spring.

Figure 1. The view of the steel tank structure.

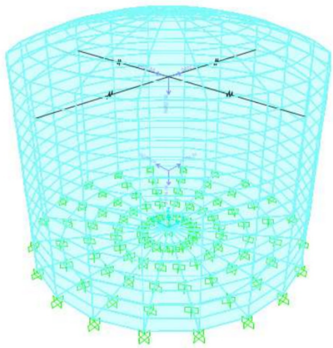

Figure 2. The structure of tank and mass-spring system of the fluid.

$$k_1 = 5.4 \frac{M_1^2}{M} \frac{gh}{R^2} \quad (5)$$

Tank structure and the fluid in the tank are shown in Fig. 2. Impulsive mass and sloshing mass are determined by using Equation 1 and Equation 2. These masses are located in the h_1 and h_2 heights. The springs showing rigidity are connected to the tank wall. The spring constant connecting the sloshing mass to the tank wall is obtained by Equation 5 [26, 27, 28].

Idealization of Soil Model

The soil, foundation and structure are taken into consideration in order to examine the soil-structure-interaction. Equation of motion for cylindrical foundations is shown in Equation 6. $X, \dot{X}, \ddot{X}, m, c, k$ show displacement, velocity, acceleration, mass, effective damping and stiffness respectively. Determining the impedance function K(w) of a rigid massless foundation is important in terms of studies regarding structure soil interactions. The harmonic and steady state response of a foundation, with a mass of zero, was founded. Dynamic impedance is known as the ratio between steady state force and displacement [23].

Dynamic impedance is shown in Equation 7. That is to say;

$$m\ddot{x} + c\dot{x} + kx = P(t) \quad (6)$$

$$K_v = \frac{R_v(t)}{v(t)} \quad (7)$$

In which; $R_v(t)$ is harmonic vertical force, $v(t)$: harmonic settlement of the foundation.

The dynamic force and displacement that occurs at the system exposed to the harmonic loads. Equation 7 is divided into two components and one of them is in the phase, another of them is 90 out of phase.

$$K_a(\omega) = K_{a1}(\omega) + iK_{a2}(\omega)$$
$$\mathrm{A} = \mathrm{v, h, r, h_r, t; i} = \sqrt{-1} \quad (8)$$

In Equation 8, these real and imaginary components are functions of vibration frequency. Real components depend on the stiffness and inertia of soil. Imaginery components depend on radiation and damping of material.

Harmonic excitation;

$$P(\mathrm{t}) = P_0 \exp(i\omega \mathrm{t}) \quad (9)$$

Steady state response;

$$\mathrm{x}(\mathrm{t}) = \mathrm{x}_0 \exp(i\omega \mathrm{t}) \quad (10)$$

Equation 11 is obtained by placing in Equation 7 of Equation 9 and Equation 10.

$$(\mathrm{K\text{-}mw}^2) + \mathrm{i}c\omega = \frac{\mathrm{P(t)}}{\mathrm{x(t)}} \quad (11)$$

Equation 12 is obtained from Equation 7 and Equation 11.

$$K = (\bar{K}\text{-mw}^2) + \mathrm{i}c\omega \quad (12)$$

Equation 13 and Equation 14 are obtained when comparing Equation 8 with Equation 12;

$$K_1 = \bar{K}\text{-}m\omega^2 \quad (13)$$

$$K_2 = c\omega \quad (14)$$

While the first (real) part which indicates stiffness and inertia forces of the system depends on the frequency, the second (imaginary) part indicates energy loss in the system and also depends on the frequency [23]. Stiffness and damping coefficients can change depending on the frequency of the foundation soil system. Dynamic impedance factor depending on the frequency is found in equation 15 [23].

$$\mathrm{K} = \bar{K}(\mathrm{k} + \mathrm{i}\omega c_s) \quad (15)$$

Viscous damping ratio is calculated by Equation 15.

$$\beta = \frac{C}{C_{Cr}} = \frac{C}{2K/\omega_n} \quad (16)$$

In Equation 17, K indicates impedance function, k stiffness and c damping.

$$K = \bar{K}(\mathrm{k} + \mathrm{i}\, a_0\, \mathrm{c}) \quad (17)$$

Dimensionless frequency factor is calculated by equation 18. In this equation, the angular frequency is indicated by w, radius for the circular foundation by B and shear wave velocity by V_s.

$$a_0 = \frac{\omega B}{V_S} \quad (18)$$

Spring system equivalent having 6 degrees of freedom is used to examine the soil-structure interaction. In the Gazetas soil model, the soil is modeled with springs and 3 translations and 3 rotations are created. The spring stiffness values $K_x, K_y, K_z, K_{\varnothing x}, K_{\varnothing y}, K_{\varnothing z}$ are calculated by using the equations in the literature. Here, r indicates the radius of the

Table 1. Equivalent lumped parameters for circular foundation [23].

Direction	Spring Stiffness
Vertical	$K_z = \frac{4Gr_z}{(1-\vartheta)}$
Horizontal	$K_x = \frac{32\ (1-\vartheta)Gr_x}{(7-8\vartheta)}$
Rocking	$K_{\varnothing x} = \frac{8Gr_{\varnothing x}{}^3}{3(1-\vartheta)}$
Rocking	$K_{\varnothing y} = \frac{8Gr_{\varnothing y}{}^3}{3(1-\vartheta)}$
Torsion	$K_{\varnothing z} = \frac{16Gr_{\varnothing y}{}^3}{3}$

Table 2. Characteristics of material in soils.

Soil	Modülüs of Elasticity (MPa)	Unit volume weight (KN/m³)
Soil 1	Fixed support	
Soil 2	400	24
Soil 3	80	20
Soil 4	40	18
Soil 5	25	18

Table 3. The properties of earthquakes [30]

Earthquake Number	Earthquake Name	Year	Vs30 (m/s)	Focus Depth (km)	Earthquake Magnitude	Soil Class	Station Name
1	Imperial Valley-06	1979	205.78	24.6	6.53	D	Calipatria Fire Station
2	Imperial Valley-06	1979	205.63	3.95	6.53	D	El Centro Array #5
3	Victoria, Mexico	1980	471.53	14.37	6.33	C	Cerro Prieto
4	Morgan Hill	1984	729.65	14.84	6.19	C	Gilroy - Gavilan Coll.
5	N. Palm Springs	1986	344.67	4.04	6.06	D	North Palm Springs
6	Whittier Narrows-01	1987	245.06	20.79	5.99	D	Downey - Birchdale
7	Loma Prieta	1989	380.89	8.5	6.93	C	Saratoga - Aloha Ave
8	Northridge-01	1994	380.06	8.44	6.69	C	LA - Sepulveda VA Hospital
9	Kobe, Japan	1995	312	0.27	6.90	D	Takarazuka
10	Northwest China-03	1997	240.09	17.73	6.10	D	Jiashi
11	Parkfield-02, CA	2004	522.74	4.08	6.00	C	Parkfield - Cholame 2E

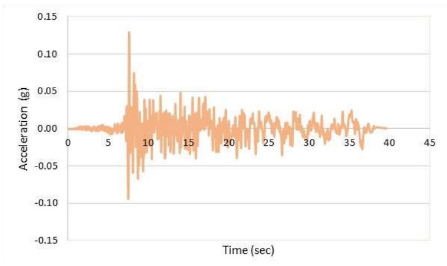

Earthquake Number 1

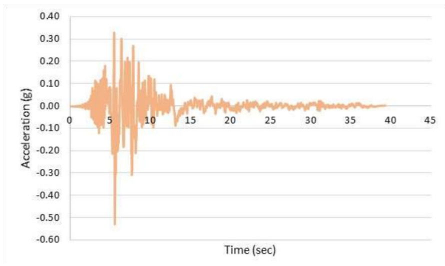

Earthquake Number 2

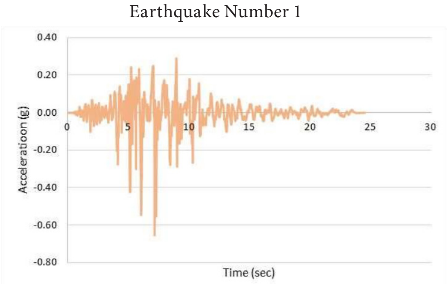

Earthquake Number 3

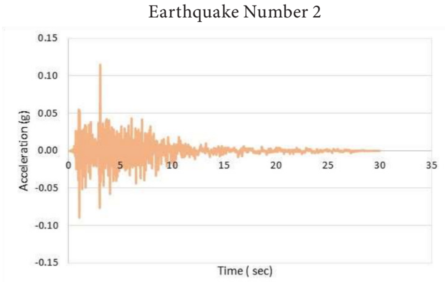

Earthquake Number 4

Figure 3. The acceleration values depending on time.

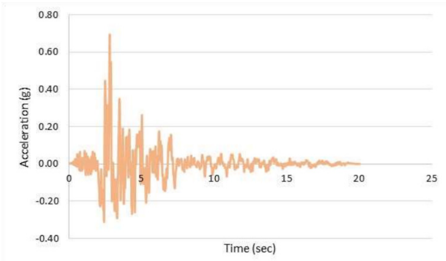

Earthquake Number 5

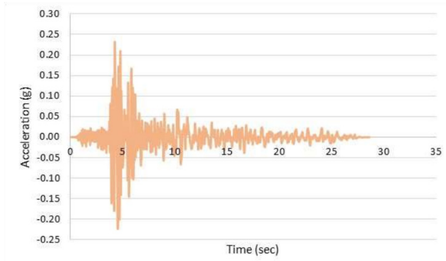

Earthquake Number 6

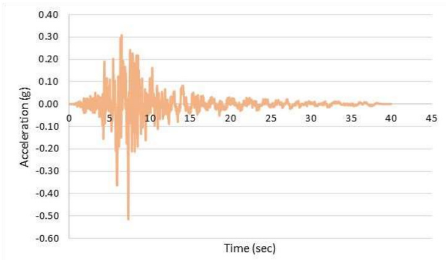

Earthquake Number 7

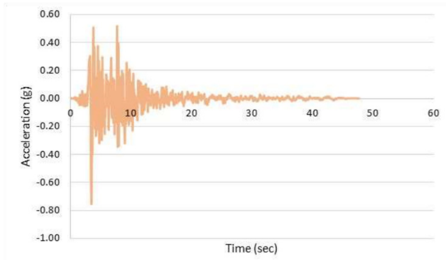

Earthquake Number 8

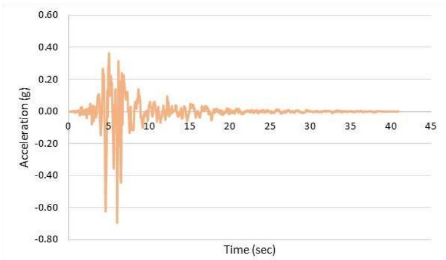

Earthquake Number 9

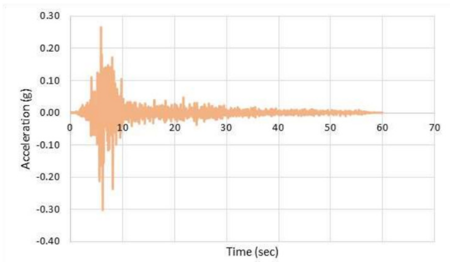

Earthquake Number 10

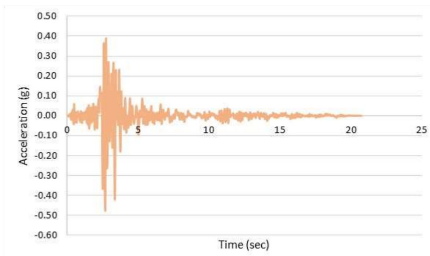

Earthquake Number 11

Figure 3. The acceleration values depending on time (continued).

circular foundation, G indicates the shear modulus of soil, , ϑ indicates poisson rate. The stiffness formulas for circular foundations and the material properties of soil is available in Table 1 and Table 2 respectively [23].

Seismic Risk Evaluation of Tank Structure

In order to perform seismic analysis of steel tank building, the time history method was used by considering fixed base and 4 different soil profiles. In this study, the effect of soil–foundation-structure interaction of tank buildings is examined by using ground motions of eleven earthquakes which occurred in the past and have different properties. The effective ground velocities of the earthquakes used in the analysis range from 205.63 m/s to 729.65 m/s, the magnitude of their range from 5.99 to 6.93 and the depth of focus their range from 0.27 km to 24.6 km. The characteristics of earthquakes and acceleration values depending on time are shown in Table 3 and Fig. 3 respectively.

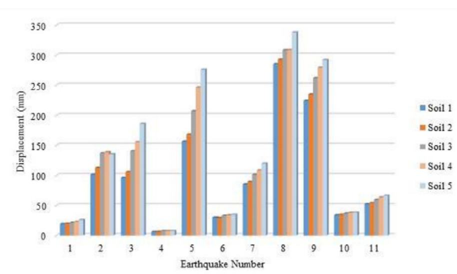

Figure 4. The values of displacement for all earthquakes and soil situations.

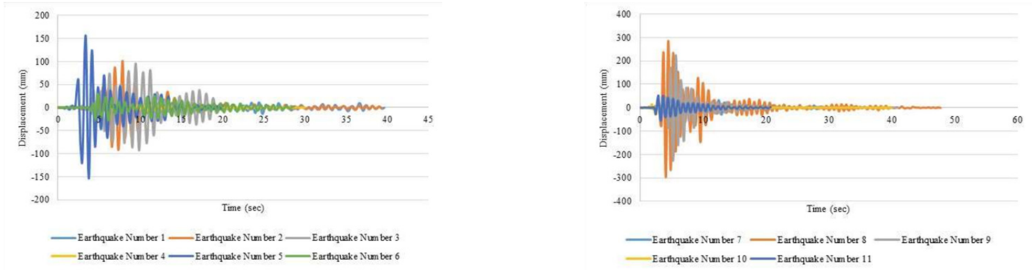

(a) Soil Type 1

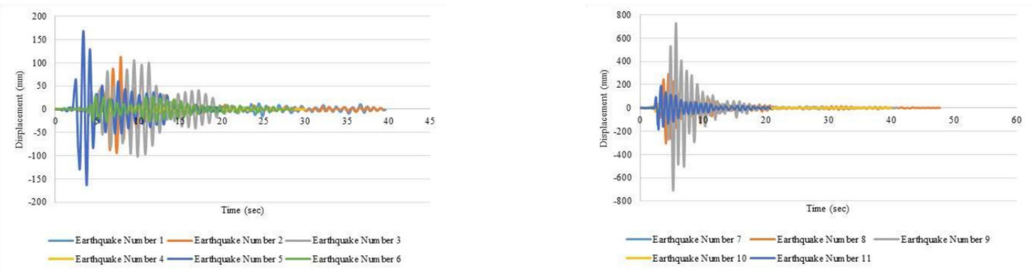

(b) Soil Type 2

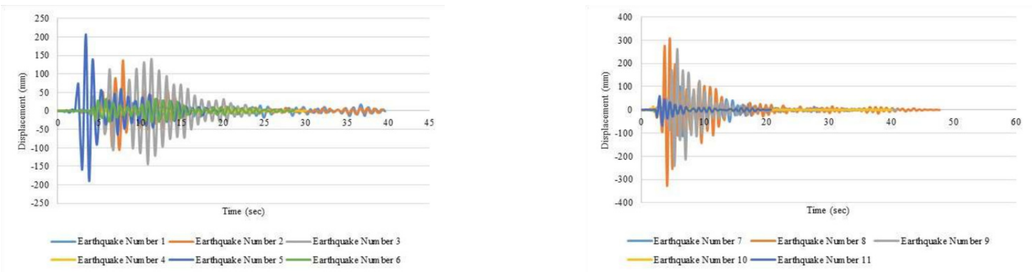

(c) Soil Type 3

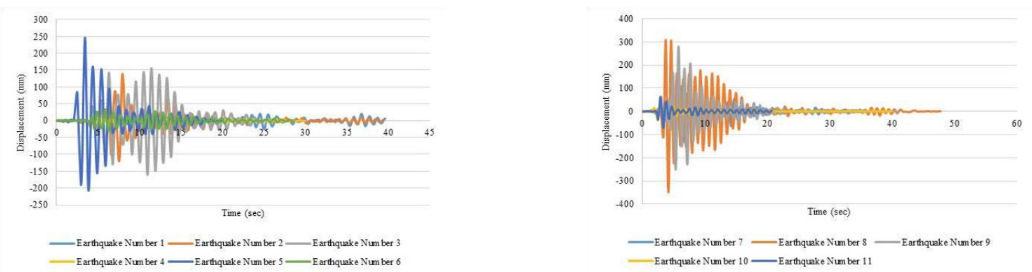

(d) Soil Type 4

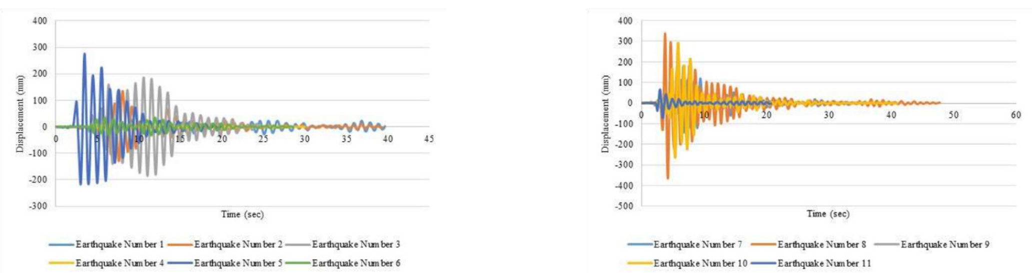

(e) Soil Type 5

Figure 5. The values of displacement depend on time for all earthquakes a) Soil Type 1 b) Soil Type 2 c) Soil Type 3 d) Soil Type 4 e) Soil Type 5.

As it is shown in Table 3, Magnitudes of 1 numbered Imperial Valley-06 (Calipatria Fire Station) Earthquake and 2 numbered Imperial Valley-06 (El Centro Array #5) earthquake are 6.53. While the peak ground acceleration of the 1 numbered Imperial Valley-06 (Calipatria Fire Station) Earthquake is 0.129g, the peak ground acceleration of the 2 numbered Imperial Valley-06 (El Centro Array #5) earthquake is 0.529g, and the ground speed is 205.78 m/s in the 1 numbered Imperial Valley-06 (Calipatria Fire Station) earthquake and is 205.63 m/s in the 2 numbered Imperial Valley-06 (El

Centro Array #5) earthquake. In view of 2 earthquakes, the focus depth of 2 numbered Imperial Valley-06 (El Centro Array #5) earthquake, which has high peak ground acceleration, has the lower than 1 numbered Imperial Valley-06 (Calipatria Fire Station) earthquake. As is seen in the Figure 2, duration of earthquakes and the values of the peak ground acceleration are different. As a result of time history analysis, displacement, stress and base shear force values were obtained and compared for eleven different earthquake conditions for each soil type.

Earthquakes were selected in accordance with TBDY 2018 [29]. The earthquake magnitudes, fault distances, local ground conditions were taken into account during earthquake selection. C and D were chosen as the soil class, and the magnitude of the earthquakes were selected between 5.99 and 6.93. 11 earthquake records having different effective ground acceleration values were used by taking from Pacific Earthquake Engineering Research Center [30].

The earthquake whose focus depth among the selected earthquakes is the smallest is 9 numbered Kobe earthquake and the earthquake whose focus depth is the largest is 1 numbered Imperial Valley-06. The distance to the fault of the center where the earthquake was recorded must be less than 10 km in order to be able to be a near fault. and the velocity pulse duration must be greater than 1.0 second, the ratio of the maximum velocity value to the maximum acceleration value must be greater than 0.1 second. [31,32,33].

RESULTS AND DISCUSSION

Determining seismic behavior of tanks is of great significance for decreasing damages which may occur in the course of the earthquake. For this purpose, a steel tank structure is designed by considering 4 soil conditions having different features and fixed support. While determining the behavior of the tank structure under the earthquake effect, dynamic analyzes were carried out with the time history method by considering the earthquakes 1979 Imperial Valley-06 (Calipatria Fire Station), 1979 Imperial Valley-06 (El Centro Array 5), Victoria, Mexico 1980, Morgan Hill 1984, N. Palm Springs 1986, Whittier Narrows-01 1987, Loma Prieta 1989, Northridge-01 1994, Kobe 1995, Northwest China-03 1997, Parkfield-02 2004.

Since the highest displacement values occur at the top of the tank, the displacement values at the top point are taken. The displacement values obtained as a result of the analysis are shown in Fig. 4. The lowest displacement values are obtained in fixed support for all earthquake conditions. The values of the largest displacement were obtained in 8 numbered Northridge-01 earthquake as 285.4372 mm, 292.7811 mm, 308.4658 mm, 308.63 mm, 337.8845 mm respectively for soil 1, soil 2, soil 3, soil 4 and soil 5. The smallest displacement values were obtained in 4 numbered Morgan Hill 1984 earthquake respectively 6.00 mm, 6.00 mm, 7.33 mm, 7.27 mm and 7.46 mm for soil 1, soil 2, soil 3, soil 4 and soil 5.

The change of displacement values depending on time for all earthquakes is shown in Figure 5. The displacement values increase with the increase in tank height. The variation depending on time is shown by taking the highest values in the top point of the tank. When analyzed in terms of earthquakes, it is seen that the displacement values are the highest in Northridge-01 earthquake, of which magnitude, peak ground velocity and focus depth are respectively 6.69, 380.06 cm/s and 8.44 km. Ankastre mesnet durumunda; 285.4372 mm yer değiştirmenin en büyük değeri elde edilmiştir. In the case of fixed support, the highest value of the displacement was obtained as 285.4372 mm. The smallest displacement value is obtained in Morgan Hill 1984 earthquake which has a magnitude of 6.19. Bu depremin yer hızı, odak derinliği sırasıyla 729.65 cm/s ve 14.84 km'dir. The ground speed, focal depth of this earthquake are respectively 729.65 cm/s ve 14.84 km. The smallest displacement value obtained is 6.00 mm. The magnitudes of 1 numbered Imperial Valley-06 (Calipatria Fire Station) and 2 numbered Imperial Valley-06 (El Centro Array #5) Earthquakes are the same, but their values of peak ground acceleration are different. The peak ground speed, depth of focus of the 1 numbered Imperial Valley-06 (Calipatria Fire Station) earthquake are respectively 205.78 cm/s, 24.6 km, while the peak ground speed and depth of focus of 2 numbered Imperial Valley-06 (El Centro Array #5) earthquake are 205.63 cm/s and 3.95 km respectively. It is seen that the values obtained from the 1 numbered Imperial Valley-06 (Calipatria Fire Station) earthquake are lower than the values obtained from 2 numbered Imperial Valley-06 (El Centro Array #5) earthquake. Peak ground velocity and focus depth of 9 numbered Kobe earthquake are 312 cm/s and 0.27 km, respectively, and it is seen that the values obtained from 9 numbered Kobe earthquake are lower than 8 numbered Northridge-01 (1994) earthquakes. The highest value of displacement obtained by using 9 numbered Kobe earthquake is 224.1925mm.

When considering the soils, the displacement graph depending on time is available in Fig. 6. It is seen that the lowest displacement values in the structure are obtained in the case of fixed support for all earthquakes. It is seen that the highest values are obtained in the case of Soil 5. The displacement value of 337.8845 mm in soil 5, 292.7811 mm in soil 2 and 285.4372 mm in the fixed support condition are obtained in 8 numbered earthquake having the highest peak ground acceleration and ground velocity. While the displacement value obtained as 6.00 mm and 6.00 mm in fixed support and in the case of soil 2, respectively, in 4 numbered Morgan Hill (1984) Earthquake, of which peak ground acceleration is the lowest, it was respectively obta-

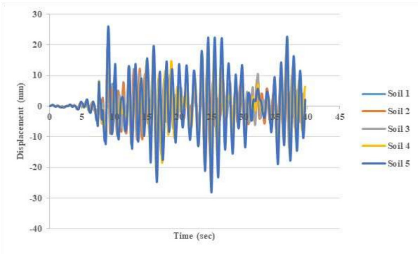

(a) Earthquake Number 1

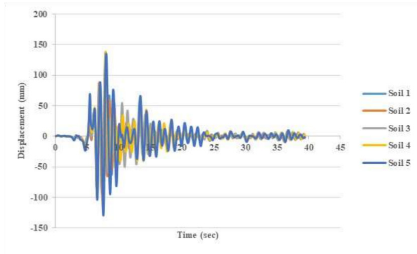

(b) Earthquake Number 2

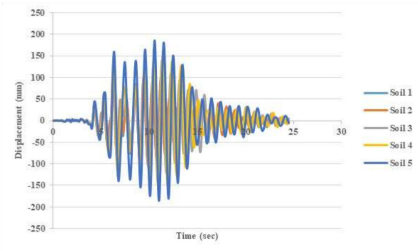

(c) Earthquake Number 3

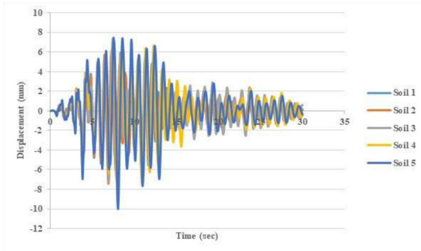

(d) Earthquake Number 4

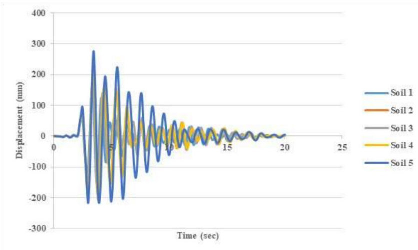

(e) Earthquake Number 5

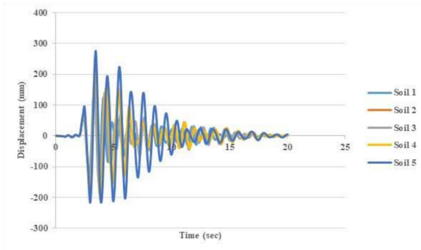

(f) Earthquake Number 6

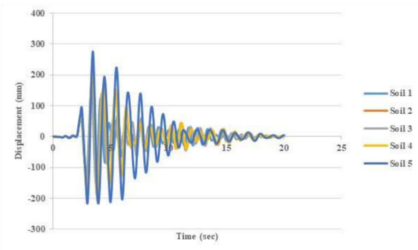

(g) Earthquake Number 7

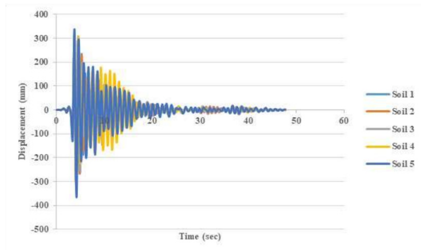

(h) Earthquake Number 8

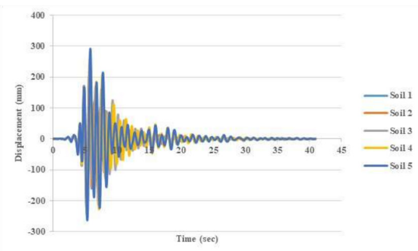

(i) Earthquake Number 9

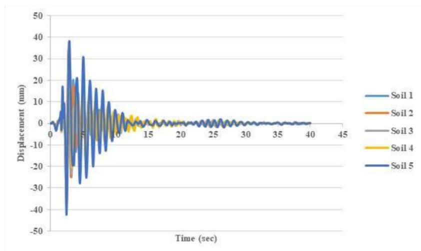

(j) Earthquake Number 10

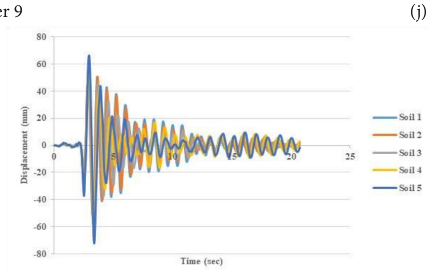

(k) Earthquake Number 11

Figure 6. The values of displacement depend on time a) Earthquake numbered 1, b) Earthquake numbered 2, c) Earthquake numbered 3, d) Earthquake numbered 4, e) Earthquake numbered 5, f) Earthquake numbered 6, g) Earthquake numbered 7, h) Earthquake numbered 8, i) Earthquake numbered 9, j) Earthquake numbered 10, k) Earthquake numbered 11 .

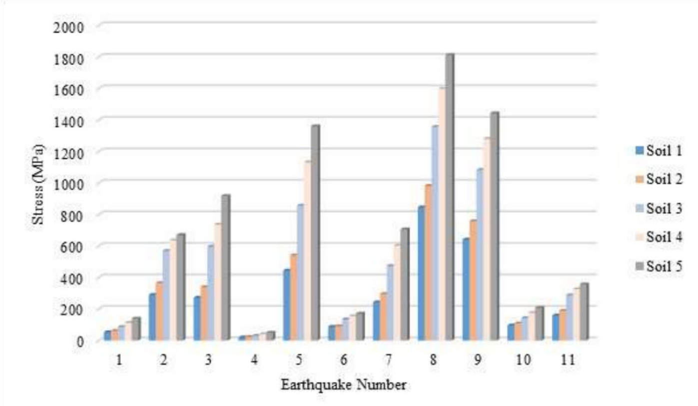

Figure 7. The values of stress for all earthquakes and soil situations.

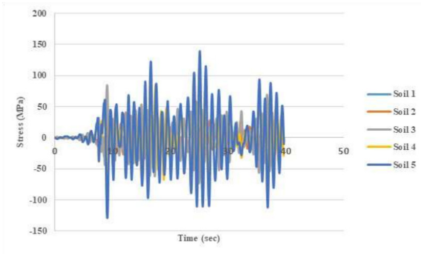

(a) Earthquake Number 1

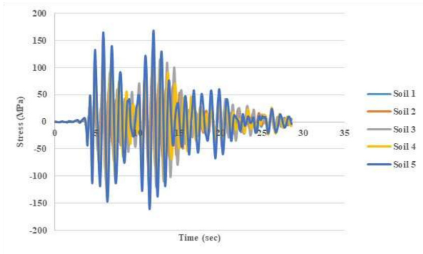

(b) Earthquake Number 2

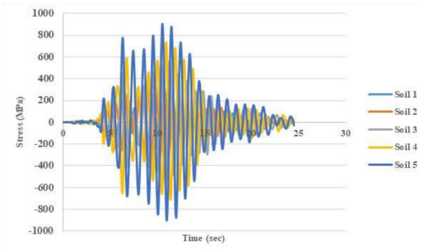

(c) Earthquake Number 3

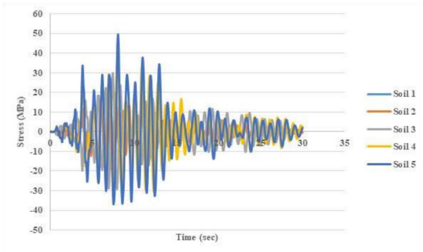

(d) Earthquake Number 4

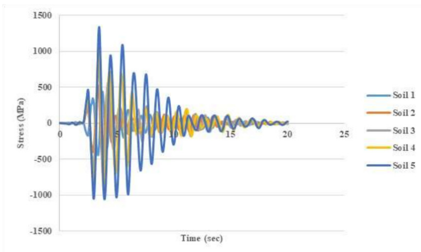

(e) Earthquake Number 5

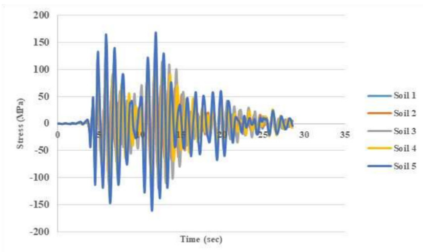

(f) Earthquake Number 6

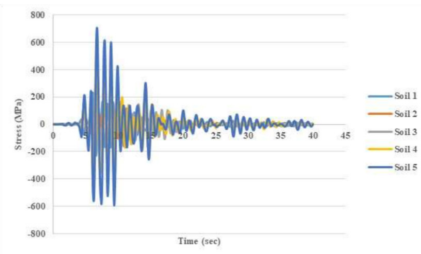

(g) Earthquake Number 7

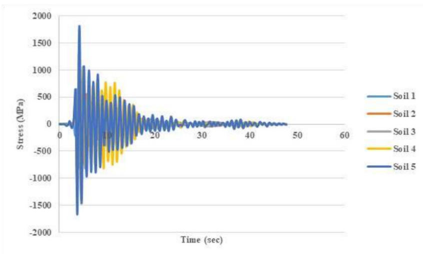

(h) Earthquake Number 8

Figure 8. The values of stress depend on time a) Earthquake numbered 1, b) Earthquake numbered 2, c) Earthquake numbered 3, d) Earthquake numbered 4, e) Earthquake numbered 5, f) Earthquake numbered 6, g) Earthquake numbered 7, h) Earthquake numbered 8, i) Earthquake numbered 9, j) Earthquake numbered 10, k) Earthquake numbered 11.

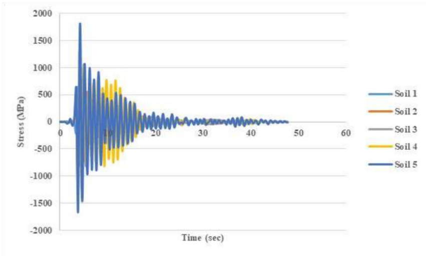

(i) Earthquake Number 9

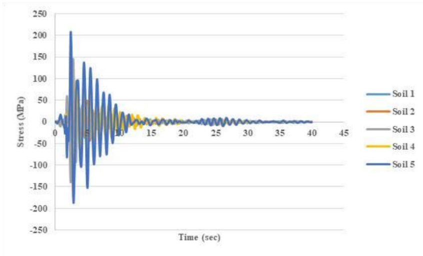

(j) Earthquake Number 10

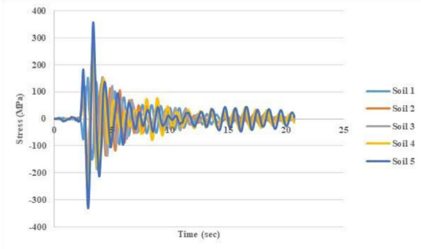

(k) Earthquake Number 11

Figure 8. The values of stress depend on time a) Earthquake numbered 1, b) Earthquake numbered 2, c) Earthquake numbered 3, d) Earthquake numbered 4, e) Earthquake numbered 5, f) Earthquake numbered 6, g) Earthquake numbered 7, h) Earthquake numbered 8, i) Earthquake numbered 9, j) Earthquake numbered 10, k) Earthquake numbered 11 (continued).

ined as 7.33mm,7.27mm, 7.45mm for the cases of soil 3,4 and 5. This value was obtained as 19.1135 mm, 19.1135mm, 21.04114mm, 22.77467mm, 26.07037mm for the cases of soil 1,2,3,4 and 5, respectively, at 1 numbered earthquake. When the 2 numbered earthquake was examined, the displacement values are obtained as 101.4455 mm, 112.8003 mm, 136.8489 mm, 138.6545mm, 135.2876 mm in cases of soil 1,2,3, 4 and 5, respectively. It is seen that the values obtained in the case of fixed support of the soil and in the case of 400 Mpa, where the elasticity module of the soil is the highest, are very similar and that the displacement values increase with the decrease of the modulus of elasticity and strength.

The values of the maximum stress and the stress depending on time are respectively seen in Fig. 7 and Fig. 8. The highest stress values were obtained as 846.265 MPa, 982.413 MPa, 1355.734 Mpa, 308.63 Mpa, 337.8845 MPa respectively in the cases of soil 1,2,3,4 and 5 at 8 numbered Northridge-01 earthquake. The smallest values of stress were obtained as 20.162 MPa, 20.162 MPa, 30.747 MPa, 40.903 MPa, 49.55 MPa respectively in the cases of soil 1,2,3,4 and 5 at 4 numbered Morgan Hill Earthquake. The ground speed of the Morgan Hill earthquake is 729.65 m/s, its focal depth is 14.84 km, its effective ground speed is 0.115 g, and it has the highest ground velocity and the smallest effective ground acceleration within11 earthquakes. The smallest displacement and stress values were obtained from this earthquake.

CONCLUSION

Examining of structure-soil-interaction of industrial structures such as tanks, silos and cooling towers to be built on weak grounds is very important in terms of structural safety. This study aims to evaluate the interaction of soil-foundation-structure having different parameters. The tank structures constructed on different soils must have required strength to stand the external loads such as earthquakes. For this purpose, the stiffness values of soils having different strengths were determined by using formulas related to elastic springs in the literature. Tank constructed on the soil designed as elastic spring was modeled with finite element methods and the dynamic analyses were performed by applying 11 time-dependent acceleration values.

The damage occuring because of the earthquakes having high peak ground acceleration and ground velocity values, are bigger compared to other earthquakes. It is seen that the effect of an earthquake having low focus depth, is higher and the damage to the structure is also bigger. When the varies of displacement and stress values depending on the time are examined, it is seen that the displacement and stress values are at the highest level at earthquake whose the value of the peak ground acceleration is at the highest level. While the highest values among these earthquakes were occurred in 8 numbered Northridge-01 earthquake, which has the highest peak ground acceleration and ground velocity values, it is followed by 9 numbered Kobe, 5 numbered N. Palm Springs, 2 numbered Imperial Valley-06 (El Centro Array #5), 3 numbered Victoria, Mexico, 7 numbered Loma Prieta, 11 numbered Parkfield-02, CA, 10 numbered Northwest China-03, 6 numbered Whittier Narrows-01, 1 numbered Imperial Valley-06 (Calipatria Fire Station) , 4 numbered Morgan Hill. The ground velocity of 4 numbered Morgan Hill earthquake has the highest and the its effective ground acceleration is the lowest. The smallest displacement and stress values were obtained in the 4 numbered Morgan Hill earthquake and the highest values were obtained in the 8 numbered Northridge-01 earthquake.

When considering different soil conditions, it is seen that the values of the displacement and stress obtained are very similar for the case in which the elasticity module of the soil is 400MPa and in the case where the soil is fixed supported. When all earthquake records were examined, it was seen that the smallest values were obtained in the case of the fixed soil and the obtained values in the soil 2, soil 3, soil 4 and soil 5 conditions respectively followed by the obtained values in fixed soil situation. It is also seen that the obtained values increase as the soil strength decreases.

CONFLICT OF INTEREST

Authors approve that to the best of their knowledge, there is not any conflict of interest or common interest with an institution/organization or a person that may affect the review process of the paper.

References

1. USGS Circular 1193. Implications for Earthquake Risk Reduction in the United States from the Kocaeli Turkey Earthquake of August 17, 1999; 2000.
2. Palanci M, Kayhan AH, Demir A. A statistical assessment on global drift ratio demands of mid-rise RC buildings using code-compatible real ground motion records. Bulletin of Earthquake Engineering. 16 (11) (2018) 5453-5488.
3. Yazici G, Cili F. Evaluation of the liquid storage tank failures in the 1999 Kocaeli Earthquake. In Proceedings of the 14th World Conference on Earthquake Engineering, Beijing, China, pp. 12-17, 2008 January.
4. Saatcioglu M, Mitchell D, Tinawi N, Gardner NJ, Gillies AG, Ghobarah A, Anderson, DL, Lau D. The August 17, 1999, Kocaeli (Turkey) earthquake - damage to structures. Can. J. Civ. Eng. 28 (2001) 715-737.
5. Kianoush M, Ghaemmaghami A. The effect of earthquake frequency content on the seismic behavior of concrete rectangular liquid tanks using the finite element method incorporating soil-structure interaction. Eng. Struct. 33 (7) (2011) 2186-2200.
6. Chung MA, Larkin TJ. Nonlinear Foundation Response of Liquid Storage Tanks under Seismic Loading. Proceedings of New Zealand Society for Earthquake Engineering Annual Conference. 2008.
7. Kramer SL. Geotechnical earthquake engineering. Prentice Hall, Upper Saddle River; 1996.
8. Veletsos AS, Meek JW. Dynamic behaviour of building foundation systems. Earthq. Eng Struct Dyn. 3 (1974) 121–38.
9. Scarfone R, Morigi M, Conti R. Assessment of dynamic soil-structure interaction effects for tall buildings: A 3D numerical approach. Soil Dynamics and Earthquake Engineering. 128 (2020) 105864.
10. Mezaini N. Effects of soil-structures interactions on the analysis of cylindrical tanks. ASCE Practice Periodical on Structural Design and Construction. 11 (1) (2006) 50–57.
11. Bhattacharya K, Dutta SC. Assessing lateral period of building frames incorporating soil-flexibility. Journal of Sound and Vibration. 269 (3-5) (2004) 795-821.
12. Dutta CH, Bhattacharya K, Roy R. Response of low rise buildings under seismic ground excitation incorporating soil structure interaction. Soil Dyn. Earthq. Eng. 24 (2004) 893–914.
13. Ghandil M, Behnamfar F. A near-field method for dynamic analysis of structures on soft soils including inelastic soil-structure interaction. Soil Dynamics and Earthquake Engineering. 75 (2015) 1–17.
14. Meng X, Li X, Xu X. Earthquake Response of Cylindrical Storage Tanks on an Elastic Soil. J. Vib. Eng. Technol. 7 (2019) 433-444.
15. Dutta S, Mandal A, Dutta SC. Soil–structure interaction in dynamic behavior of elevated tanks with alternate frame staging configurations. Journal of Sound and Vibration, 227 (4-5) (2004) 825-853.
16. Zhao C, Chen J, Wang J, Yu N, Xu Q. Seismic mitigation performance and optimization design of NPP water tank with internal ring baffles under earthquake loads. Nuclear Engineering and Design, 318 (2017) 182-201.
17. Zhao C, Chen J, Xu Q. FSI effects and seismic performance evaluation of water storage tank of AP1000 subjected to earthquake loading. Nuclear Engineering and Design. 280 (2014) 372-388.
18. Nicolici S, Bilegan RM. Fluid structure interaction modeling of liquid sloshing phenomena in flexible tanks. Nuclear Engineering and Design, 258 (2013) 51-56.
19. Patel CN, Sharma, K, Patel HS. Modeling of Soil-Structure Interaction as Finite Element Using Using SAP2000. 2011.
20. Seleemah, AA, El-Sharkawy M. Seismic analysis and modeling of isolated elevated liquid storage tanks. Earthquake and Structures, 2 (4) (2011) 397-412.
21. Livaoğlu R, Doğangün A. Simplified seismic analysis procedures for elevated tanks considering fluid–structure–soil interaction. Journal of fluids and structures, 22 (3) (2006) 421-439.
22. Livaoglu, R. and Dogangün A. Seismic behaviour of cylindrical elevated tanks with a frame supporting system on various subsoil. Indian Journal of Engineering & Materials Sciences 14 (2007) 133-145.
23. Gazetas G. Analysis of machine foundation vibrations: state of the art. International Journal of Soil Dynamics and Earthquake Engineering. 2 (1) (1983) 2-4.
24. Habibullah and Wilson. SAP 2000 User Manual, Computer Program, Computers and Structures. Berkeley, USA.1998.
25. Roder HM. Liquid Densities of Oxygen, Nitrogen, Argon and Parahydrogen (Metric Supplement), Cryogenic Division, Institute for Basic Standards (U.S.). National Bureau of Standards, Technical Note 361; 1974.
26. Housner GW. The dynamic behavior of water tanks. Bulletin of the seismological society of America, 53 (2) (1963) 381-387.
27. Housner GW. Dynamic pressures on accelerated fluid containers. Bulletin of the seismological society of America, 47 (1) (1957) 15-35.
28. Jacobsen LS. Impulsive hydrodynamics of fluid inside a cylindrical tank and of fluid surrounding a cylindrical pier. Bulletin of the Seismological Society of America, 39 (3) (1949) 189-204.
29. TBDY, Türkiye Bina Deprem Yönetmeliği, Ankara,2018.
30. Pacific Earthquake Engineering Research (PEER) Center, https://ngawest2.berkeley.edu/
31. Akkar S, Yazgan U, Gülkan P. Drift estimates in frame buildings subjected to near-fault ground motions. Journal of Structural Engineering, 131 (7) (2005) 1014-1024.
32. Kayabalı, K. Geoteknik Deprem Mühendisliği, Gazi Kitabevi, Ankara, 2003.
33. Özmen A. Yakın ve uzak fay hareketlerine maruz tarihi yığma bir köprünün sismik performansının değerlendirilmesi, Fırat Üniversitesi, Fen Bilimleri Enstitüsü, 2019.